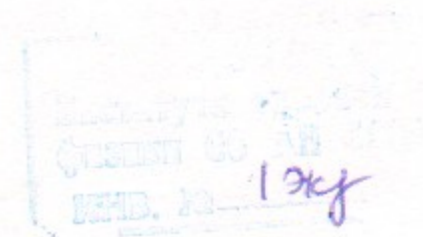A.29

Sh.Zh. Akhmadaliev, G.Ya. Kezerashvili,
S.G. Klimenko, R.N. Lee, V.M. Malyshev,
A.L. Maslennikov, A.M. Milov, A.I. Milstein,
N.Yu. Muchnoi, A.I. Naumenkov, V.S. Panin,
S.V. Peleganchuk, G.E. Pospelov,
I.Ya. Protopopov, L.V. Romanov,
A.G. Shamov, D.N. Shatilov, E.A. Simonov,
V.M. Strakhovenko, Yu.A. Tikhonov

EXPERIMENTAL INVESTIGATION
OF HIGH-ENERGY PHOTON SPLITTING
IN ATOMIC FIELDS

Novosibirsk
2001

Sh.Zh. Akhmadaliev, G.Ya. Kezerashvili, S.G. Klimenko,
R.N. Lee,V.M. Malyshev, A.L. Maslennikov, A.M. Milov,
A.I. Milstein, N.Yu. Muchnoi, A.I. Naumenkov, V.S. Panin,
S.V. Peleganchuk, G.E. Pospelov, I.Ya. Protopopov,
L.V. Romanov, A.G. Shamov, D.N. Shatilov,
E.A. Simonov, V.M. Strakhovenko, Yu.A. Tikhonov

EXPERIMENTAL INVESTIGATION OF HIGH-ENERGY PHOTON SPLITTING IN ATOMIC FIELDS.

Budker INP 2001-80

Experimental investigation of high-energy photon splitting in atomic fields.

Sh.Zh. Akhmadaliev, G.Ya. Kezerashvili, S.G. Klimenko,
R.N. Lee, V.M. Malyshev, A.L. Maslennikov, A.M. Milov,
A.I. Milstein, N.Yu. Muchnoi, A.I. Naumenkov, V.S. Panin,
S.V. Peleganchuk, G.E. Pospelov, I.Ya. Protopopov,
L.V. Romanov, A.G. Shamov, D.N. Shatilov,
E.A. Simonov, V.M. Strakhovenko, Yu.A. Tikhonov

Budker Institute of Nuclear Physics
630090 Novosibirsk, Russia

Abstract

The new data analysis of the experiment, where the photon splitting in
the atomic fields has been observed for the first time, is presented. This
experiment was performed at the tagged photon beam of the ROKK-1M
facility at the VEPP-4M collider. In the energy region of 120-450 MeV , the
statistics of $1.6 \cdot 10^9$ photons incident on the BGO target was collected. About
400 candidates to the photon splitting events were reconstructed. Within
the attained experimental accuracy, the experimental results are consistent
with the cross section calculated exactly in an atomic field. The predictions
obtained in the Born approximation significantly differ from the experimental
results.

1. Introduction

Photon splitting is a process where the initial photon turns into a virtual
electron-positron pair which scatters in the electric field of an atom and then
transforms into two photons sharing the initial photon energy ω_1. This is
an example of a self-action of an electromagnetic field, which results also in
such effects as coherent photon scattering (Delbrück scattering) and photon-
photon scattering. The latter phenomenon was never observed experimen-
tally.

Delbrück scattering was investigated in detail both theoretically and ex-
perimentally [1–3]. It turned out that, for heavy atoms and high photon
energy, its cross section calculated exactly in the parameter $Z\alpha$ ($Z|e|$ is the
nucleus charge, $\alpha = e^2/4\pi = 1/137$ is the fine-structure constant) drasti-
cally differs from that obtained in the lowest order in this parameter (Born
approximation).

Recently, an essential progress in understanding of photon splitting phe-
nomenon was achieved. In papers [4–6] various differential cross sections of
high-energy photon splitting have been calculated exactly in the parameter
$Z\alpha$. Similar to the case of Delbrück scattering, the exact cross section turns
out to be noticeably smaller than that obtained in the Born approximation.
So, the detailed experimental investigation of photon splitting provides a new
sensitive test of QED when the effect of higher-order terms of the perturbation
theory with respect to the external field is very important.

The observation of photon splitting is a difficult problem due to a small-
ness of its cross section as compared to those of other processes initiated
by photons in a target. The following background processes are significant:
double Compton effect off the atomic electrons ($\gamma e \to \gamma\gamma e$), and the emis-
sion of two hard photons from e^+e^- pair produced by the initial photon.
The relative importance of these processes depends on the photon energy.
For the energy $\omega_1 \sim m$, where the search of photon splitting was under-
taken in two experiments [7,8], only double Compton scattering determines
the background conditions. In these experiments, the photons from an in-
tense radioactive source (Zn^{65} with $\omega_1 \simeq 1.1$ MeV in [7], and Co^{60} with
$\omega_1 \simeq 1.17, 1.33$ MeV in [8]) were used. The combination of the coinci-
dence and energy-summing detection technique was applied. The number of
events considered as candidates for photon splitting exceeded the theoretical
expectations by the factor of 300 in [8], and by the factor of 6 in [7].

At high photon energy $\omega \gg m$ the emission of hard photons from e^+e^-
pair becomes most important as a background process. In 1973 the experi-
ment devoted to the study of Delbrück scattering of photons in energy region

$1 \div 7$ GeV was performed [9]. The bremsstrahlung non-tagged photon beam was used. Some events were assigned by authors of [9] to the photon splitting process. As shown in [10,11], the theoretical value for the number of photon splitting events under the conditions of the experiment was two orders of magnitude smaller than the experimental result. It was also argued that the events observed could be explained by the production of e^+e^- pair and one hard photon.

The first successful observation of photon splitting was performed in 1995-96 using the tagged photon beam of the energy $120 \div 450$ MeV at the VEPP-4M e^+e^- collider [12] in the Budker Institute of Nuclear Physics (Novosibirsk). Another goal of this experiment was a study of Delbrück scattering [3]. The total statistics collected was $1.6 \cdot 10^9$ incoming photons with BGO (bismuth germanate) target and $4 \cdot 10^8$ without target for background measurements. The preliminary results were published in [13], [14]. Here we present the new data analysis for this experiment.

2. Scheme of experiment

The experimental setup is shown in Fig. 1. Some ideas of this setup were suggested in [15]. The main features of the experimental approach are:

- The use of high-quality tagged photon beam produced by backward Compton scattering of laser light off high-energy electron beam. Thereby, the energy of the initial photon is accurately determined.

- Strong suppression of the background processes by means of the detection of charged particles produced in the target and in other elements of the photon-beam line.

- The detection of both final photons to discriminate the photon splitting events from those with one final photon produced in Compton or Delbrück scattering.

- The requirement of the balance between the sum of the energies of the final photons and the energy of the tagged initial photon. This provides the additional suppression of the events with charged particles missed by the detection system.

At high energy of the initial photon $\omega_1 \gg m$, the photon splitting cross section is peaked at small angles between momenta of all photons ($\sim m/\omega_1$). Therefore, a good collimation of the primary photon beam is required. The

ROKK-1M facility [16] is used as the intense source of the tagged γ-quanta. The electron energy loss in the process of Compton scattering of laser light is measured by the tagging system (TS) [17] of the KEDR detector [18]. The TS consists of the focussing spectrometer formed by accelerator quadrupole lenses, bending magnets, and 4 hodoscopes of the drift tubes. High-energy photons move in a narrow cone around the electron beam direction. The angular spread is of the order $1/\gamma$, where $\gamma = E_{beam}/m$ is the relativistic factor of the electron beam. The photon energy spectrum has a sharp edge at

$$\omega_{th} = \frac{4\gamma^2 \omega_{laser}}{1 + 4\gamma\omega_{laser}/m}, \qquad (1)$$

that allows one to perform the absolute calibration of the tagging system in a wide energy range. In experiment the laser photon energy was $\omega_{laser} = 1.165$ eV, the electron beam energy $E_{beam} = 5.25$ GeV, and $\omega_{th} = 450$ MeV. The photon energy resolution provided by the tagging system depends on the photon energy and on the position of scattered electron in TS hodoscope: it was 0.8 % at $\omega_1 = 450$ MeV (at the center of the hodoscope) and ~ 5 % at $\omega_1 = 120$ MeV (at the edge of the hodoscope). The collimation of the photon beam is provided by two collimators spaced at 13.5 m. The last collimator, intended to strip off the beam halo produced on the first one, is made of four BGO (bismuth germanate) crystals as shown in the separate view in Fig. 1. After passing through the collimation system, the photon beam hits $1X_0$ thick BGO crystal target. In order to separate the photons passed the target without interaction from those scattered in the target, certain angular region around the photon beam direction ($\theta \leq 2.4$ mrad) was enclosed by the dump. It is made of 13 X_0 thick BGO crystal installed in front of the photon detector. The only photons to be detected are those scattered outside the dump shadow. All active elements used in the beam line (collimators, target, dump, scintillating veto counter) set a veto signal in the trigger and their signals are used in the analysis for background suppression. The information from the target and beam dump is also used for measurement of the incoming photon flux. The liquid-krypton ionization calorimeter is used for the detection of the final photons. Its three-layer double-sided electrode structure enables one to get both (X and Y) coordinates for detected photons. The energy resolution of the calorimeter is $2\%/\sqrt{\omega(\text{GeV})}$. The liquid-krypton calorimeter is described in details in [19,20].

In the experiment, the detected final photons had the polar angles in the region 2.4 mrad $\leq \theta \leq 20$ mrad. The corresponding cross section is called "visible". Fig. 2 shows the calculated energy dependence of the total (a)

and visible (b) cross sections for various processes initiated by photons in BGO target: e^+e^- pair production, Compton scattering on atomic electrons, Delbrück scattering, and photon splitting. The calculation of the photon splitting cross section was performed using the results obtained in [4–6].

3. Results

In the event selection procedure the following constraints were applied:

- The absence of the signal caused by charge particles in all active elements of the photon-beam line.

- The balance of the tagged initial photon energy and the energy measured in the calorimeter within 3σ of its energy resolution.

- The existence of two separate tracks at least for one (X or Y) coordinate in the calorimeter strip structure. The track is found if there are close clusters in different layers.

The fulfillment of the latter requirement strongly suppresses the contribution of the processes with one photon in the final state which could imitate two photon events in the calorimeter.

The typical event which meets selection criteria is shown in Fig. 3. In this example two tracks are seen in both X and Y directions. The conversion of the first photon occurs in the Layer 1 while the second photon converts in the Layer 2.

The experimental results are presented in Tab. 1 and in Figs. 4, 5 together with the results of Monte-Carlo simulation based on the exact photon splitting cross section. The energy spectrum of the initial photons measured in the tagging system is shown in Fig.4(a). Tab. 1 and Fig. 5 present the data summed up over the initial photon spectrum. The errors shown in the Table are statistical ones. The systematic error is determined by the accuracy of the measurement of the number of initial photons and by the uncertainty in the reconstruction efficiency of photon splitting events. The estimation of these systematic errors gives 2 % and 5 %, respectively.

As seen from the Table 1 and Fig. 5a, the main part of the photon splitting events has, in agreement with the theory, a complanarity angle φ (the azimuth angle between final photon momenta) close to 180°. The choice of the interval $\varphi > 150°$ allows us to improve the signal-to-background ratio (see, e.g., the last two rows of the Table 1). Just this φ-interval was used to plot the distributions over polar angles in Fig. 5 and the dependence of the number

Table 1. The number of reconstructed events meeting the selection criteria. Here Q is the number of incoming photons. The quantity $N_{\varphi<150°}$ is the number of events with the complanarity angle $\varphi < 150°$ (see Fig. 5), $N_{\varphi>150°}$ is the number of events with $\varphi > 150°$. The quantities $N_{\varphi<150°}$ and $N_{\varphi>150°}$ are normalized to the experimental statistics collected with the target. MC means Monte-Carlo simulation.

DATA	TARGET	Q, 10^9	$N_{\varphi>150°}$	$N_{\varphi<150°}$
Experiment	$Bi_4Ge_3O_{12}$	1.63	336±18	82±9
Experiment	no target	0.37	10±3	10±3
MC photon splitting	$Bi_4Ge_3O_{12}$	6.52	364±10	72±5
MC Delbrück scattering	$Bi_4Ge_3O_{12}$	1.63	2±1	16±4
MC other backgrounds	$Bi_4Ge_3O_{12}$	1.63	0	16±4

of reconstructed photon splitting events on the initial photon energy E_{TS} in Fig. 4(b). Note that for most of the events in this φ-interval, the variable $\tilde{x} = \theta_{min}/(\theta_{min} + \theta_{max})$ is approximately equal to the ratio $\min(\omega_2, \omega_3)/\omega_1$ since the main contribution to the cross section comes from the region $|\mathbf{k}_{2\perp} + \mathbf{k}_{3\perp}| \ll k_{2\perp}, k_{3\perp}$, i.e. $\varphi \approx 180°$ and $\omega_2\theta_2 \approx \omega_3\theta_3$.

The results presented in the Table 1 and in Figs. 4(b), 5 show a good agreement between the theory and the experiment. More precisely, the total number of reconstructed events in the experiment (see Table 1) differs from the result of MC simulation by 1.5 standard deviations.

In order to demonstrate the role of the Coulomb corrections under the experimental conditions, we show in Fig. 6 the visible cross sections calculated exactly in $Z\alpha$ and in the Born approximation as a function of the initial photon energy. For all energies considered, the Born result exceeds the exact one by 20 % approximately. Therefore, the use of the Born cross section for MC simulation would lead to the disagreement between the theory and the experiment of 3.5 standard deviations. In other words, the experimental results are significantly closer to predictions of the exact theory than to those obtained in the Born approximation.

4. Conclusion

The results obtained confirm the existence of photon splitting phenomenon. They also make possible the quantitative comparison with the theoretical predictions. Moreover, the attained experimental accuracy allows one to distinguish between the theoretical predictions obtained with or without accounting

ing for the Coulomb corrections. It turns out that the Coulomb corrections essentially improve the agreement between the theory and the experiment. We conclude that the experiment and the theory are consistent within the achieved experimental accuracy.

Acknowledgments

References

[1] P.Papatzacos and K.Mork, Phys. Rep. 21 (1975) 81.

[2] A.I.Milstein and M.Schumacher, Phys. Rep. 243 (1994)183.

[3] Sh.Zh.Akhmadaliev et al., Phys. Rev. C 58 (1998) 2844.

[4] R.N.Lee, A.I.Milstein, and V.M.Strakhovenko, Zh. Éksp. Teor. Fiz. 112 (1997) 1921 [JETP 85 (1997) 1049].

[5] R.N.Lee, A.I.Milstein, and V.M.Strakhovenko, Phys.Rev. A 57 (1998) 2325.

[6] R.N.Lee, A.I.Milstein, and V.M.Strakhovenko, Phys.Rev. A 58 (1998) 1757.

[7] A.W.Adler and S.G.Cohen, Phys. Rev. 146 (1966) 1001.

[8] W.K.Roberts and D.C.Liu, Bull. Amer. Phys. Soc., 11 (1966) 368.

[9] G. Jarlskog et al., Phys. Rev. D 8 (1973) 3813.

[10] V.N.Baier, V.M.Katkov, E.A.Kuraev and V.S.Fadin, Phys.Lett. B 49 (1974) 385.

[11] R.M. Dzhilkibaev et al., JETP Lett. 19 (1974) 47.

[12] V.V. Anashin et al., "Proceedings of the VII Russian Workshop on Charged Particle Accelerators", Dubna, 1980, 246.

[13] Sh. Zh. Akhmadaliev et al., PHOTON'97, Incorporating the XIth International Workshop on Gamma-Gamma Collisions, Egmond-aan-Zee, Netherlands, 246 (10-15/05/97).

[14] A.L. Maslennikov "Photon physics in Novosibirsk", Workshop on photon interactions and the photon structure, Lund, 1998, 347-365.

[15] A.I.Milstein, B.B.Wojtsekhovski, It is possible to observe photon splitting in a strong Coulomb field, Preprint BINP 91-14, Novosibirsk, 1991.

[16] G.Ya. Kezerashvili et al., Nucl. Inst. Meth. B 145 (1998) 40.

[17] V.M. Aulchenko et al., Nucl. Inst. Meth. A 355 (1995) 261

[18] V.V. Anashin et al., "Proceedings of the International Symposium on Position Detectors in High Energy Physics", Dubna, 1988, 58

[19] V.M. Aulchenko et al., Nucl. Inst. Meth. A 394 (1997) 35

[20] V.M. Aulchenko et al., Nucl. Inst. Meth. A 419 (1998) 602-608

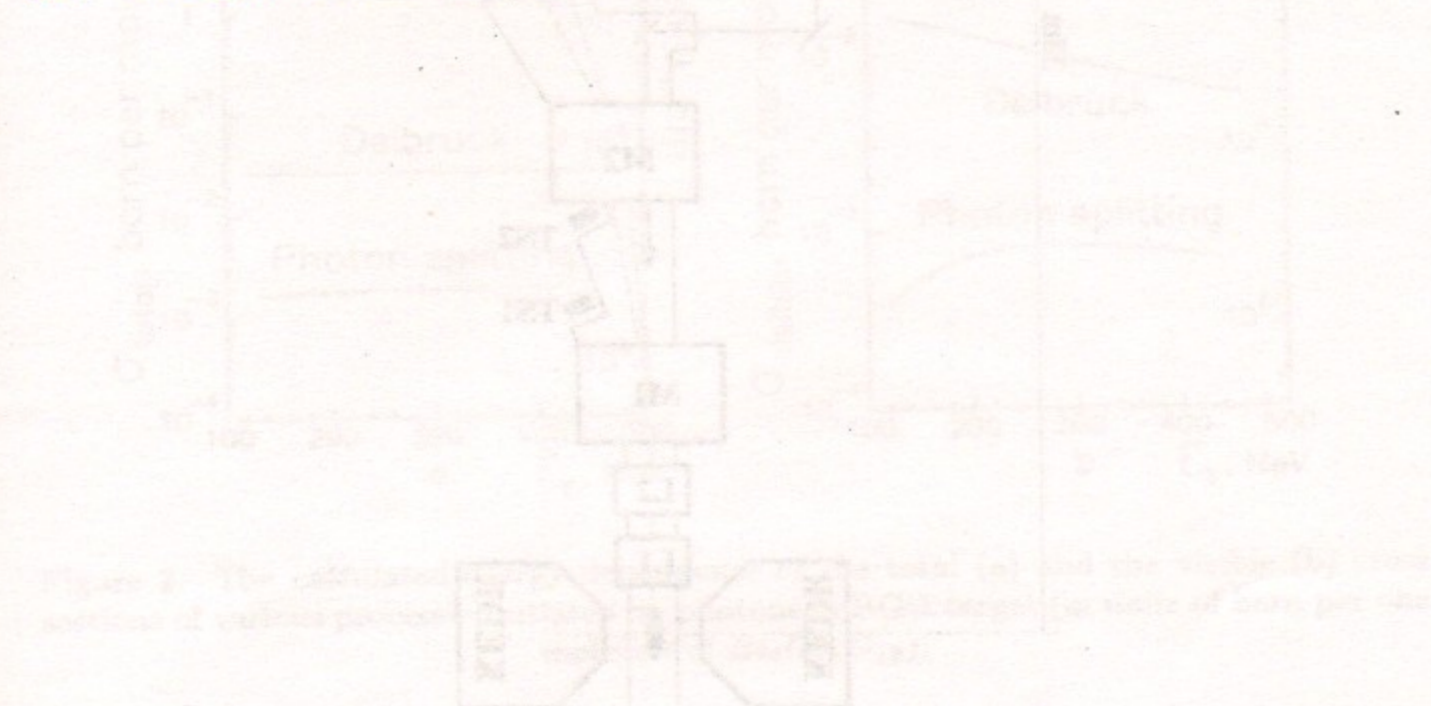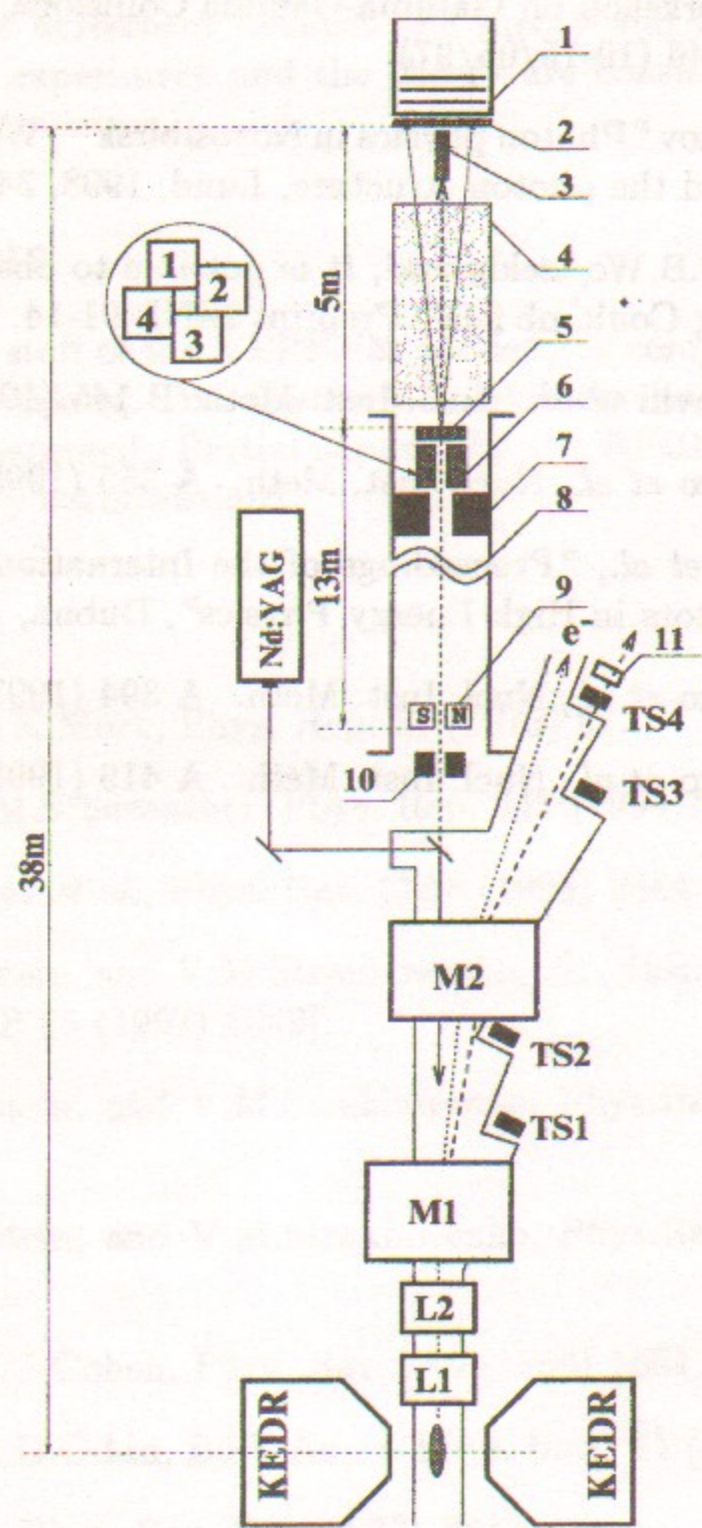Figure 1. Principal scheme of setup: LKr calorimeter (1); scintillation veto-counter (2); beam dump (BGO) (3); He-filled tube (4m length) (4); target (BGO) (5); active collimator (BGO) (6); lead absorber (7); guiding tube for the gamma-quanta beam (8); cleaning magnet (9); passive lead collimator (10); TS scintillation counter (11); Nd:YAG is the laser; TS1-TS4 are tagging system hodoscopes; M1 and M2 are bending magnets; L1 and L2 are quadrupole lenses.
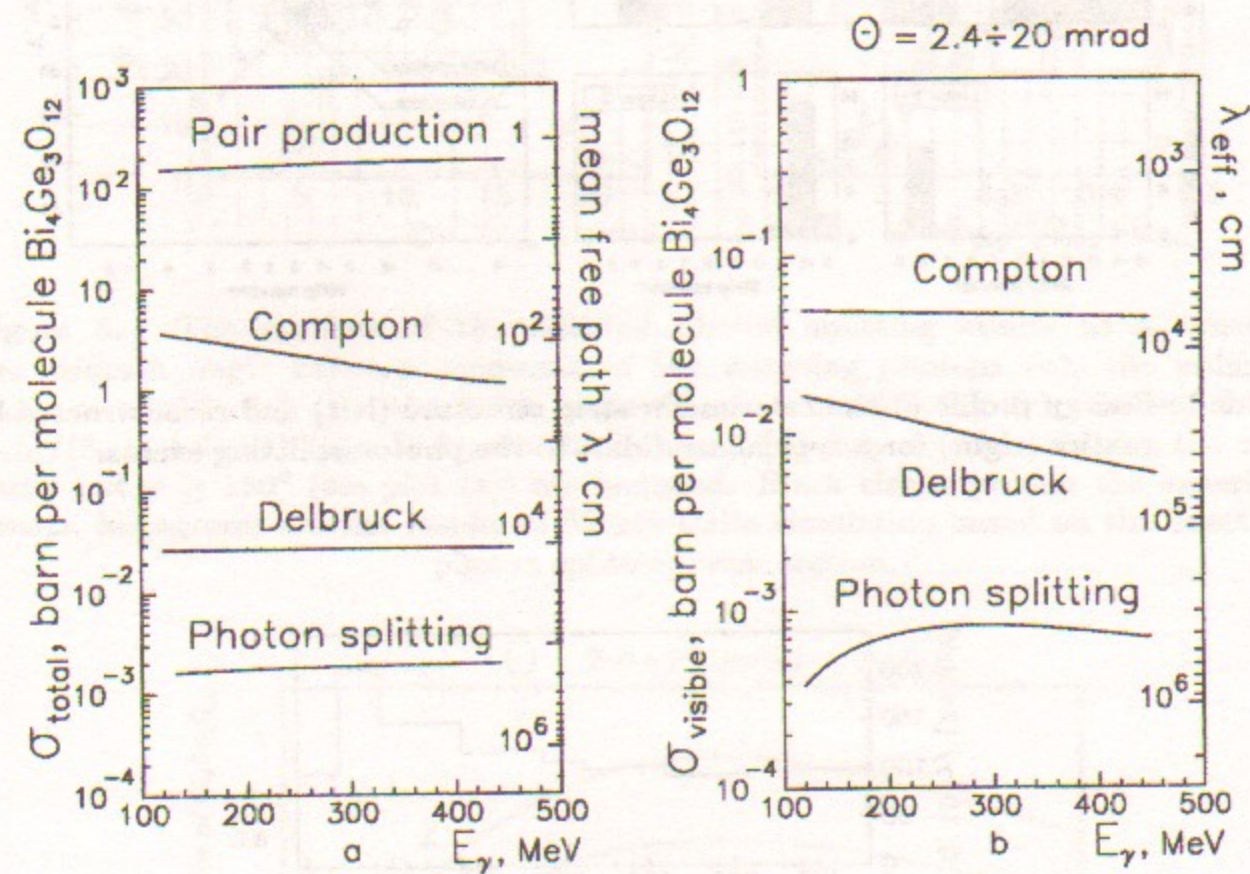

Figure 2. The calculated energy dependence of the total (a) and the visible (b) cross sections of various processes initiated by photons in BGO target (in units of barn per one molecule of $Bi_4Ge_3O_{12}$).
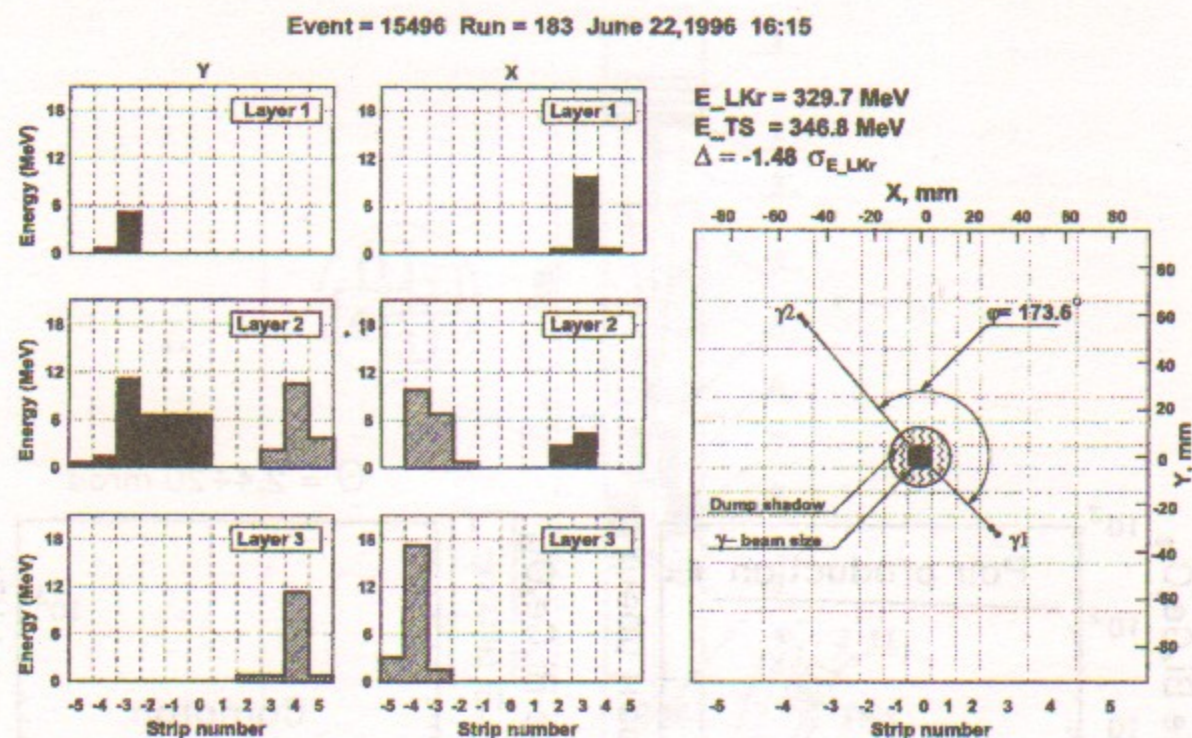
Figure 3. Energy profile in the calorimeter strip structure (left) and reconstructed kinematics (right) for a typical candidate to the photon splitting events.
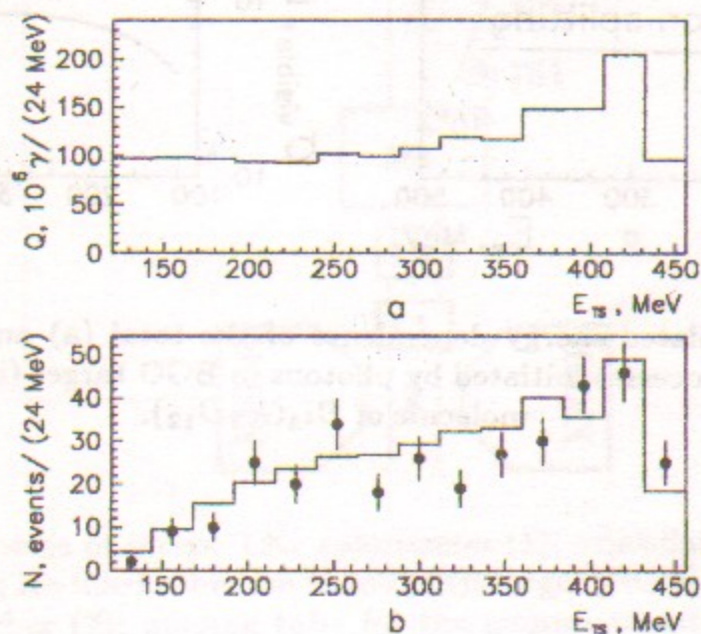

Figure 4. (a) The photon energy spectrum measured in the tagging system (TS). (b) The number of reconstructed photon splitting events as a function of the tagged photon energy E_{TS}. In plot b black circles present the experimental results, histogram is the result of Monte-Carlo simulation based on the exact in $Z\alpha$ photon splitting cross section.
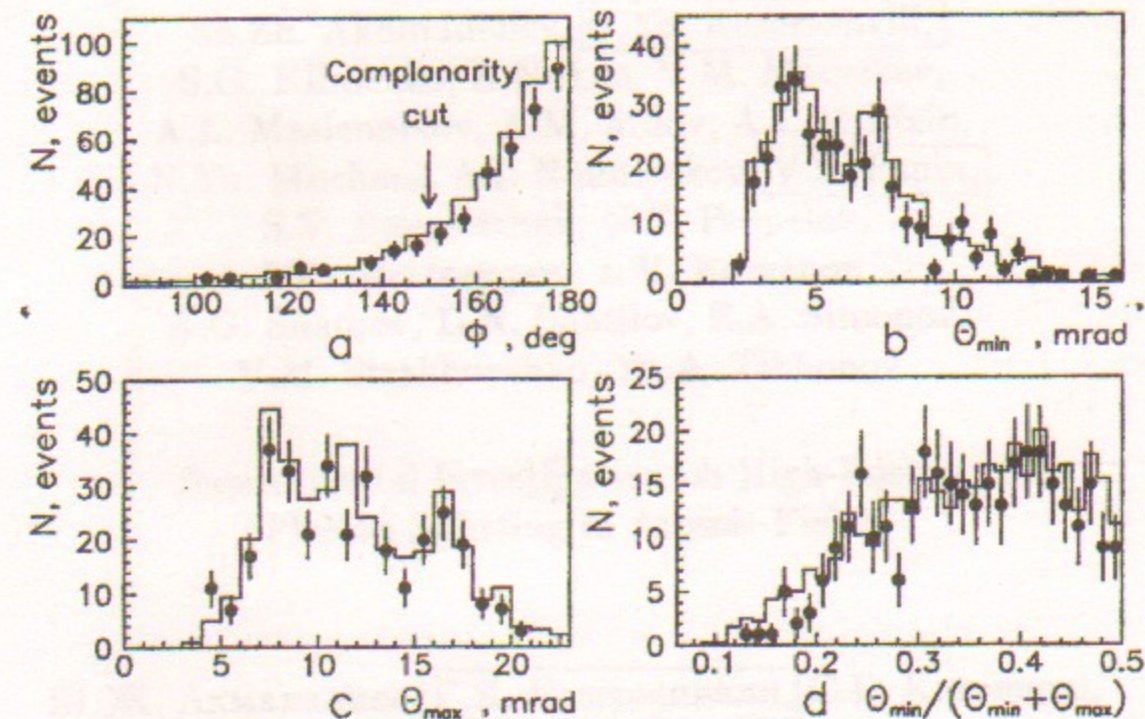

Figure 5. The number of the selected photon splitting events as a function of the azimuth angle between momenta of the outgoing photons (a), the polar angle $\theta_{min} = \min\{\theta_2, \theta_3\}$ (b), the polar angle $\theta_{max} = \max\{\theta_2, \theta_3\}$ (c), the variable $\bar{x} = \theta_{min}/(\theta_{min} + \theta_{max})$ (d). In figures (b), (c), and (d) only events satisfying the complanarity cut $\varphi \geq 150°$ (see plot (a)) are included. Black circles present the experimental results, histograms are the results of Monte-Carlo simulation based on the exact in $Z\alpha$ photon splitting cross section.
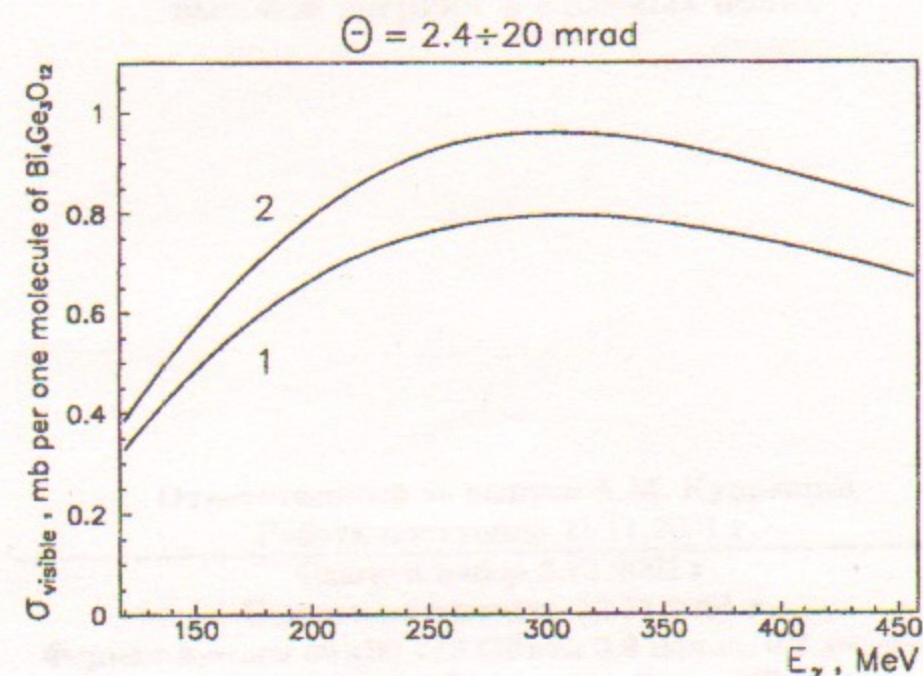

Figure 6. The visible photon splitting cross section calculated exactly in $Z\alpha$ (1) and in the Born approximation(2) as a function of the initial photon energy.

Sh.Zh. Akhmadaliev, G.Ya. Kezerashvili,
S.G. Klimenko, R.N. Lee, V.M. Malyshev,
A.L. Maslennikov, A.M. Milov, A.I. Milstein,
N.Yu. Muchnoi, A.I. Naumenkov, V.S. Panin,
S.V. Peleganchuk, G.E. Pospelov,
I.Ya. Protopopov, L.V. Romanov,
A.G. Shamov, D.N. Shatilov, E.A. Simonov,
V.M. Strakhovenko, Yu.A. Tikhonov

Experimental Investigation oh High-Energy Photon Splitting in Atomic Fields

Ш.Ж. Ахмадалиев, Г.Я. Кезерашвили, С.Г. Клименко,
Р.Н. Ли, В.М. Малышев, А.Л. Масленников, А.М. Милов,
А.И. Мильштейн, Н.Ю. Мучной, А.И. Науменко, В.С. Панин,
С.В. Пеleganчук, Г.Э. Поспелов, И.Я. Протопопов,
Л.В. Романов, А.Г. Шамов, А.Г. Шатилов, Е.А. Симонов,
В.М. Страховенко Ю.А. Тихонов

Экспериментальное исследование расщепления фотона высокой энергии в атомных полях